Journal of Renewable Materials
DOI:10.32604/jrm.2020.013353
Article

Tech Science Press

Feasibility Study on Fabrication of Geopolymer Bricks by Wasted Grinding Wheel at Room Temperature

Yi-Che Hsieh[1,*], Ta-Wui Cheng[2] and Chia-Ho Wu[2]

[1]Department of Materials and Mineral Resources Engineering, National Taipei University of Technology, Taipei, 10608, Taiwan
[2]Institute of Mineral Resources Engineering, National Taipei University of Technology, Taipei, 10608, Taiwan
*Corresponding Author: Yi-Che Hsieh. Email: v2vvv222@gmail.com
Received: 03 August 2020; Accepted: 24 August 2020

Abstract: In this study, the feasibility of producing eco-friendly bricks by using geopolymer technology and a waste grinding wheel (WGW) from the grinding wheel industries was investigated. Nowadays, in order to meet industrial needs, for instance, in Taiwan, approximately 500,000 grinding wheels are used annually. That is, a large number of "waste" grinding wheels are produced. Furthermore, few studies have been conducted on the use of WGWs as raw materials in geopolymer applications. The use of geopolymer technology to form bricks can avoid the utilization of clay and cement and even prevent the use of a high-temperature process in kilns. Moreover, it can decrease CO_2 emission and energy consumption and thus, protect the environment. In this study, the following three major factors were considered: press-forming pressure (70 and 100 kgf/cm^2), NaOH molar concentration (2 and 4M), and the ratio of binder fine-aggregate (1:3, 1:4, and 1:5). Under these conditions, the specimens were tested using the compressive strength test, water absorption test, microstructure analysis, a freezing–thawing test and toxicity characteristic leaching procedure test. The optimal formulation was composed of 1:4 binder fine-aggregate ratio, 4M NaOH concentration, and 100-kgf/cm^2 pressure. Furthermore, we used a WGW and achieved a compressive strength of 50.6 MPa after 28 days, which was greater than 32 MPa and conformed to the Grade A brick standard of National Standards of the Republic of China (13295). In conclusion, this brick fabrication method based on geopolymer technology was not only beneficial to the environment but also improved the efficiency of reutilizing WGW.

Keywords: Geopolymer; waste grinding wheel; geopolymer bricks

1 Introduction

Bricks have been used as building materials for at least 5000 years. Nowadays, for the propose of meetings the needs of urban transformation, construction, and infrastructure, approximately 1500 billion bricks are produced annually [1]. In the conventional manufacturing of bricks, fried clay, sand, and cement are utilized as source materials. Moreover, a high-temperature treatment is indispensable. However, a high temperature leads to massive energy consumption, and a considerable amount of CO_2 is emitted in the process. Therefore, the traditional high-temperature bricks are environmentally harmful. At

the same time, it has been observed that clay and cement are becoming gradually scarce in both the developing and the developed countries. For instance, China established regulations to restrict and reduce the amount of clay and cement used in brick manufacturing [2,3].

For the reasons mentioned above, to improve the conventional fabrication of bricks, various innovative types of utilization by new raw materials and in non-fired treatments have been proposed in studies recently [4–8]. According to the modus, they can be classified into two primary technologies: the high-pressure press-forming method [9–12] and the injection molding method [13–16]. Although these two methods can decrease greenhouse gas emissions, they still bring on high production costs and considerable energy consumption.

Apart from the methods mentioned above, the eco-friendly geopolymer technology [17,18], based on the use of an alkaline solution, industrial by-product, and waste, provides another method to make bricks and realizes low CO_2 emission and energy consumption in the process. Simultaneously, a geopolymer material, which has considerable durability [19] and excellent mechanical properties [20,21], is favorable for making bricks. In related studies of geopolymer bricks, several materials have been utilized, such as 800°C fired ceramic wall dust [22], waste bricks [23], residual rice husk [24], and copper mine tailing [25]. Moreover, Madani et al. [26] explored the feasibility of utilizing the wasted material of aggregates such as an alkaline solution with a different ratio of NaOH and $Ca(OH)_2$; the compressive strength of the press-forming mortar can reach 75 MPa after 4 days by curing at 105°C. Apithanyasai et al. [27] mixed electric arc furnace slag with an NaOH alkaline solution to make geopolymer bricks and cured the mixture at ambient temperature. The specimens, which were a mixture of waste foundry sand, fly ash, and electric arc furnace slag in the ratio of 40:30:30, reached the highest compressive strength value of 25.76 MPa, which was beyond the requirement of paving bricks.

Grinding wheels, composed of abrasive compounds, are used for various grinding (abrasive cutting) and abrasive machining operations. After being worn away, they are regarded as waste grinding wheels (WGWs). In this study, WGWs were used unprecedentedly as fine aggregates with geopolymer technology in brick fabrication. Meanwhile, the pressure method was adopted, and the bricks were made and cured at room temperature. Moreover, the compressive strength, water absorption, microstructure, crystal phases, freezing–thawing characteristics, and toxicity of the leaching procedure were tested and analyzed. Instead of the traditional manufacturing of bricks, this new method and raw material were put forward to improve the environment and served as the basis for the development of geopolymer bricks.

2 Experiment

2.1 Materials

In this study, the waste grinding wheel (WGW) was acquired from Kinik Company, Yingge town, Taiwan. By crushing and subsequently passing through four mesh (4760-micron) sieves, the WGW was prepared as a fine aggregate. Ground granulated blast furnace slag (GGBFS) with a D_{50} value of 12.02 μm and obtained from CHC Resources, Kaohsiung, Taiwan, was used as the binder. Fig. 1 shows the WGW and GGBFS particle size distributions. The chemical compositions of WGW and GGBFS are presented in Tab. 1. According to this table, the main components of WGW were 63.4% Al_2O_3 and 32.0% SiO_2. The GGBFS was mainly composed of 57.4% CaO and 27.3% SiO_2, and had 10.8% Al_2O_3 as well. The X-ray diffraction analysis results of WGW and GGBFS are shown in Fig. 2. The main mineral phase of WGW was corundum (Al). The amorphous phase of GGBFS contained a massive amount of glass.

The alkaline solution was a mixture of an aqueous solution of sodium hydroxide, sodium silicate, and sodium aluminate. The molar ratios of SiO_2/Na_2O and SiO_2/Al_2O were controlled at 1.28 and 50, respectively. Furthermore, 98% purity sodium hydroxide (NaOH) was provided by All Rights Reserved,

Taipei, Taiwan, and the solutions were prepared with different concentrations of 2M and 4M. In the geopolymer reaction, sodium silicate provided adequate silica and alumina to enhance the compressive strength of the product [28]; sodium aluminate supplemented the insufficient aluminum ions and increased the bonding between the aluminum and the silicon ions, resulting in a relatively dense structure, which contributed to the relatively high mechanical strength [29]. With respect to the preparation of the alkaline solution, the first step was to dissolve NaOH flakes in water for at least 5 min. Because of the heat and bubbles, the solution needed at one day to cool down to ambient temperature and defoam. Then, sodium silicate and sodium aluminate were added in order and stirred for 5 min to form an alkaline solution.

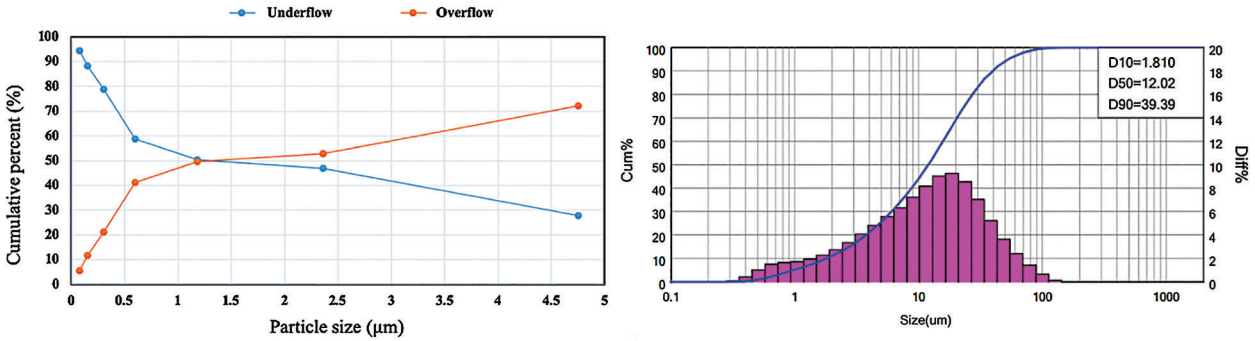

(a) (b)

Figure 1: Particle size distribution of a) WGW and b) GGBFS

Table 1: Chemical composition of materials (wt.%)

Composition	CaO	K_2O	SiO_2	TiO_2	Al_2O_3	Fe_2O_3	Others	LOI
WGW	2.1	0.6	32.0	0	63.4	0.7	1.2	0
GGBFS	57.4	0.3	27.3	1.1	10.8	0	1.3	1.8

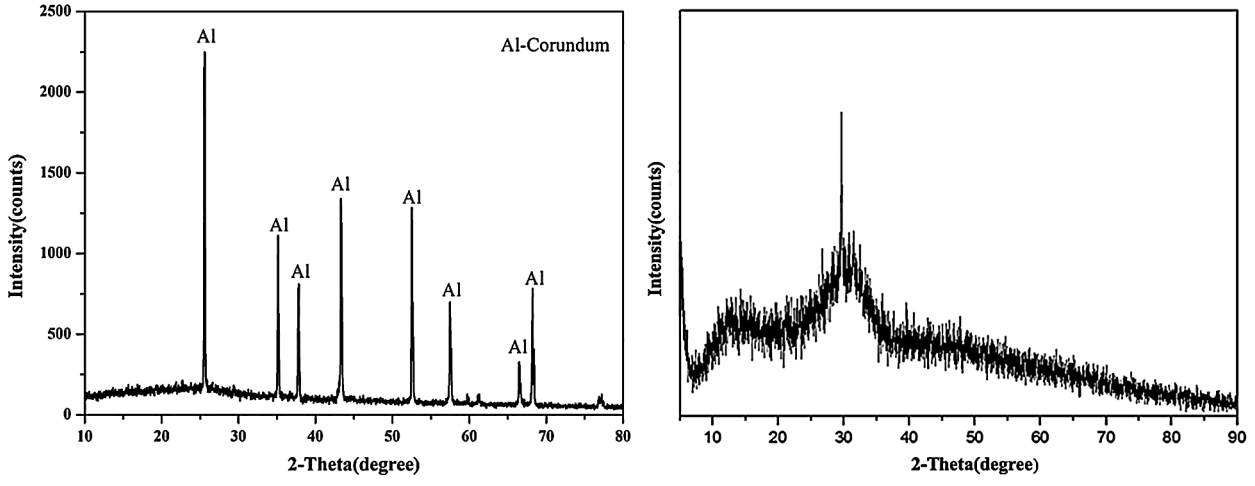

(a) (b)

Figure 2: XRD patterns of a) WGW and b) GGBFS

2.2 Experimental Method

The fabrication of geopolymer bricks was divided into three steps: (1) Mixing WGW and GGBFS for 1 min. (2) Adding the alkaline solution and mixing for another 1 min. (3) Filling the mortars in molds measuring 200 mm × 100 mm × 60 mm and then pressing them with a hydraulic compression machine to form the bricks according to the national standards of CNS 13295 [30]. After demolding, the specimens were cured at ambient temperature for 7, 14, and 28 days before the tests.

In this study, the three main influencing factors, namely forming pressure, NaOH concentration, and the ratio of binder fine-aggregate were studied. Tab. 2 shows the details of the mixing proportion for geopolymer bricks. The specimens were made using a forming pressure of 70 and 100 kgf/cm^2, NaOH molar concentration of 2 and 4, and the ratio of binder fine-aggregate of 1:3, 1:4, and 1:5. The liquid/solid ratio was controlled at 0.12.

Table 2: Mixing proportion for geopolymer bricks

Specimens label	NaOH concentration (M)	SiO_2/Na_2O	SiO_2/Al_2O_3	Liquid/Solid	GGBFS (wt.%)	WGW (wt.%)	Press-forming pressure (kgf/cm^2)
2M-1:3-100	2	1.28	50	0.12	0.75	2.25	100
2M-1:4-100	2	1.28	50	0.12	0.6	2.4	100
2M-1:5-100	2	1.28	50	0.12	0.5	2.5	100
4M-1:4-70	4	1.28	50	0.12	0.6	2.4	70
4M-1:3-100	4	1.28	50	0.12	0.75	2.25	100
4M-1:4-100	4	1.28	50	0.12	0.6	2.4	100
4M-1:5-100	4	1.28	50	0.12	0.5	2.5	100

2.3 Test Methods

2.3.1 Compressive Strength Test

In accordance with the CNS (1238 A3051) [31], to form cuboid geopolymer WGW bricks, we drilled the cylindrical specimens for the compressive strength test. As defined in CNS (9212 B7197), the constant loading rate was set as 1 mm/min [32].

2.3.2 Water Absorption Test

The water absorption and bulk specific density tests, based on Archimedes' principle, were conducted according to CNS (619 R3013) [33].

The water absorption (A_W) was calculated as follows:

$$A_W(\%) = \frac{W_{3-}W_1}{W_3 - W_2} \times 100$$

The bulk specific density (D_b) was calculated as follows:

$$D_b = \frac{W_1}{W_3 - W_2}$$

Here, W_1 denotes the weight of the specimen after complete drying at 105–120°C, W_2 represents the weight of the specimen after 24 h of soaking, and W_3 indicates the saturation weight of the specimen.

2.3.3 Microstructure Analysis

To investigate the geopolymer WGW bricks' microstructure, crystal phase, and chemical properties, a scanning electron microscopy (SEM/EDS) analysis, ZEISS Gemini SEM500; X-ray diffraction (XRD) analysis, Hitachi U-3310; and Fourier-transform infrared spectroscopy (FTIR), INVENIO; were performed.

2.3.4 Freezing–Thawing Test

In this study, the freezing–thawing test was conducted according to the FCMA-WFC-610 standard. The duration of one freezing–thawing cycle was 6 h: At the start, we set the specimens at 20–30°C ± 1°C for 1 h. Next, we increased the temperature to 50–60°C ± 1°C in 20 min and then maintained it for 1 h. Then, we decreased the temperature to 20–30°C ± 1°C in 40 min and maintained it for 1 h. Thereafter, we decreased the temperature to −10°C ± 1°C in 40 min and froze the specimens for 1 h. Finally, we increased the temperature to 20–30°C ± 1°C in 20 min. The specimens were tested 30 times in cycles, and the total testing time was 180 h. After 30 freezing–thawing cycles, the specimens were drilled for the compressive strength test to calculate the strength loss.

2.3.5 Toxicity Characteristic Leaching Procedure Test

The toxicity characteristic leaching procedure test (TCLP) was performed according to TCLP US-EPA method 1311. First, 5.7 mL of glacial acetic acid was diluted to a stable pH by adding 994.3 mL of deionized water. Second, the specimens were ground and passed through a 200-mesh (74-micron) sieve. Third, 12.5 g of the specimen powders were mixed into the solution and stirred. Fourth, we extracted 250 mL of the mixing solution and then rotated the samples for 18 h at 30 rpm with a zero-headspace extraction vessel (ZEH). Finally, we used an inductively coupled plasma mass spectrometer (ICP) with a detection limit of at least 1 ppb to determine the elemental concentrations from the mixture.

3 Results and Discussion

3.1 Compressive Strength Test Results

3.1.1 Effect of Forming Pressure

Fig. 3 shows the effect of the forming pressure on the compressive strength test. The specimens were prepared under the following conditions: 4M NaOH concentration, 1:4 binder fine-aggregate ratio, and 70- and 100-kgf/cm^2 forming pressure. Irrespective of whether the bricks were made under the pressure of 70 or 100 kgf/cm^2, the compressive strengths increased with an increase in the curing age. Under 70-kgf/cm^2 pressure, the 28-day compressive strength was 27.2 MPa; in contrast, under the pressure of 100 kgf/cm^2, the 28-day compressive strength was 50.6 MPa, which was beyond 32 MPa and conformed to the Grade A brick standard of CNS (13295). These results indicated that the forming pressure could tremendously affect the compressive strength of geopolymer bricks. Thus, we inferred that a higher forming pressure made the bricks denser and then eventually increased the density and the compressive strength [11,34].

3.1.2 Effect of NaOH Concentration and Binder Fine-Aggregate Ratio

The influence of the NaOH concentration and the binder fine-aggregate ratio on the compressive strength is shown in Fig. 4. We observed that the strength of specimens made at the NaOH concentration of 2M on day 28 reached up to 21.5–39.5 MPa, and the strength of specimens made at the NaOH concentration of 4M on day 28 reached up to 38.9–56.1 MPa. Upon the increase in the NaOH molar concentration from 2M to 4M, the compressive strength increased sharply at every curing age. The higher NaOH concentration that could increase both the reaction rate and the strength were also reported elsewhere [35–37].

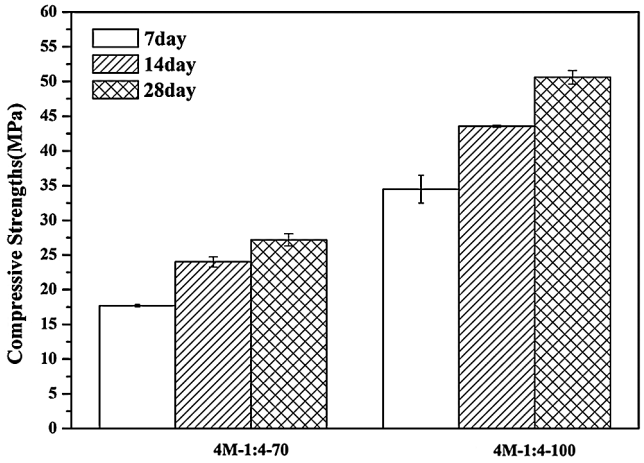

Figure 3: Effect of press-forming pressure on compressive strength test

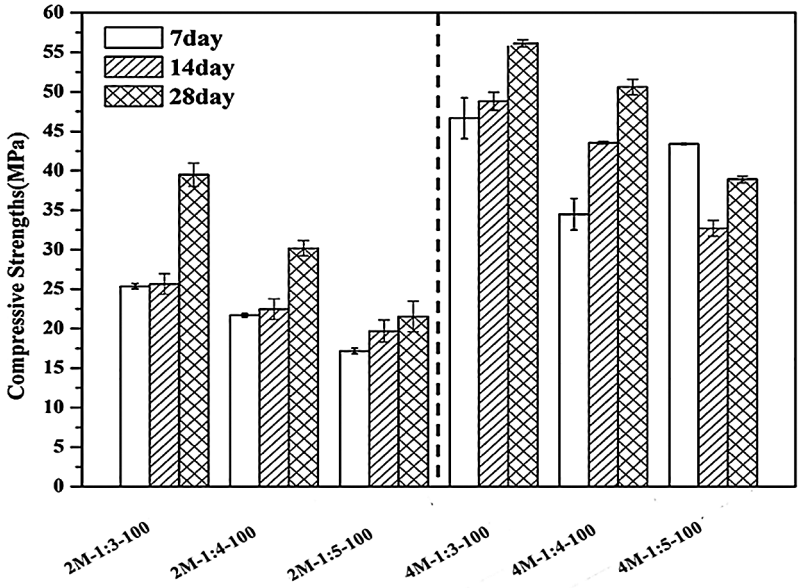

Figure 4: Effect of NaOH concentration and binder fine-aggregate ratio on compressive test

The results indicated that the compressive strengths declined in all of the specimens, followed by an increase in the fine-aggregate relative to the low content of GGBFS. This implied that overdosing fine-grained fillers deteriorated the mechanical properties of the geopolymer; to be more specific, the compressive strength of the geopolymer increased with more aggregates; however, when the aggregates added to more than 70%, the strength decreased [38,39]. Furthermore, the higher proportion of the binder material in the specimens resulted in a denser structure because the pores between the aggregates could be fully filled [40]. Therefore, because of the lacking slurry in geopolymer bricks, the compressive strength was ultimately affected in this study.

Moreover, the strength of the specimens prepared under the 4M NaOH and 1:5 binder fine-aggregate ratio fluctuated at different curing ages. Thus, we inferred that the pores between the aggregates could not be filled in the case of a low binder content, leading to unstable compressive strength.

According to the above description, only 2M-1:3-100 samples could reach the Grade A brick standard of CNS (13295) after 28 days. In contrast, the specimens prepared under the condition of 4M NaOH concentration could reach the Grade A brick standard at all the curing ages, but the strength of 4M-1:5-100 fluctuated. Furthermore, although the compressive strength of 4M-1:3-100 was 56.1 MPa, which was far higher than the Grade A brick standard, the WGW usage of 4M-1:4-100 was more than that of 4M-1:3-100. For the purpose of compliance with the standards, it was not necessary to enhance the compressive strength to as high a value as possible. That is, being up to par, the usage volume of WGW had to be increased by as many times as we could. As a result, the optimal parameters were 4M NaOH concentration and a 1:4 binder fine-aggregate ratio in this study. Specimens prepared under these conditions could reach the Grade A brick standard and had a higher WGW usage that could produce the best possible results.

3.2 Water Absorption and Bulk Density

According to the results reported above, the considerable compressive strength and high usage of WGW could be obtained at a binder fine-aggregate ratio of 1:4. As a consequence, the effect of the NaOH concentration and the forming pressure on the water absorption and the bulk density was only observed at the 1:4 binder fine-aggregate ratio, as shown in Tab. 3. The results indicated that under the 100-kgf/cm^2 pressure, both the 2M and 4M NaOH specimens had a higher bulk density than that of the specimens prepared under 70-kgf/cm^2 pressure. This was because a higher bulk density led to a lower water absorption and then finally formed denser structures. Moreover, a higher concentration of NaOH resulted in a less porous matrix, which decreased the water absorption and increased the bulk density. Accordingly, the higher forming pressure and NaOH concentration made the geopolymer bricks denser and increased the compressive strength.

Table 3: Effect of NaOH concentration and forming pressure on water absorption and bulk density

Specimen label	Water absorption (%)		Bulk density (g/cm^3)	
	7 days	28 days	7 days	28 days
2M-1:4-100	13	13	2.2	2.2
4M-1:4-70	16	14	1.9	2
4M-1:4-100	9	8	2.4	2.4

3.3 Characterization of Geopolymer WGW Bricks

Fig. 5 illustrates the SEM images and the EDS spectra of WGW and 4M-1:4-100 specimens. According to Fig. 5a, WGW was irregular and uneven and mainly consisted of Al and Si elements in the detected area. The 4M-1:4-100 specimen is presented in Fig. 5b. It was not merely composed of Al and Si elements but had the Ca element as well in the detected area.

The XRD analysis results of the WGW and 4M-1:4-100 specimens are shown in Fig. 6. Corundum was found to be the major crystal phase in both the figures. Compared with the raw WGW in Fig. 6a, the geopolymer WGW bricks in Fig. 6b reduced approximately half of the intensity. This phenomenon implied that the amorphous geopolymer slurry might be covered or surrounded by crystalline WGW. Therefore, the corundum intensity decreased. The main reaction product is shown near 29.5° 2θ. It could be attributed to the geopolymerization, coinciding with the calcium silicate hydrate gel (C–S–H) [41,42].

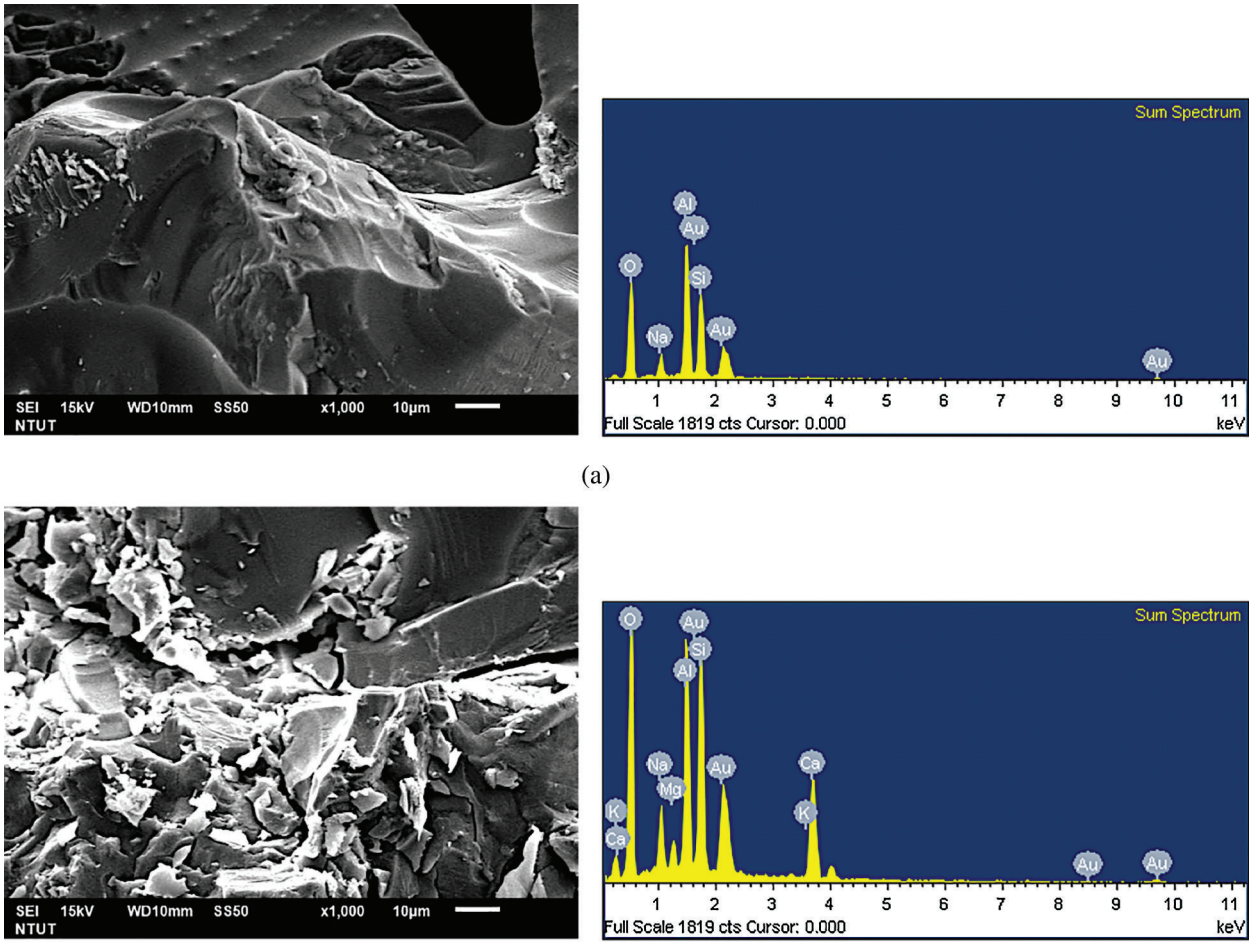

Figure 5: SEM images and EDS spectra (1000×) of a) waste grinding wheel and b) 4M-1:4-100

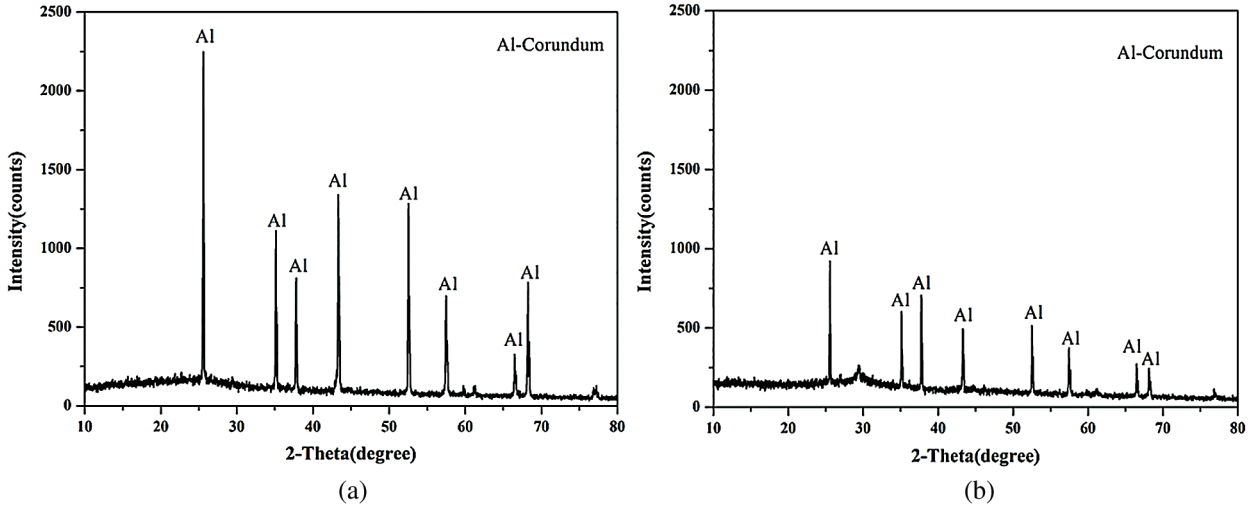

Figure 6: XRD patterns of a) WGW and b) 4M-1:4-100

The FTIR analysis results of the WGW and 4M-1:4-100 specimens are presented in Fig. 7. Apparent changes in the molecular and bond structure were observed in geopolymer WGW bricks. We observed that the bands in the range of 450–470 cm^{-1} were associated with the Si–O–T bonds from the structure of the silicate and the aluminates [43]. The peaks at approximately 1000 cm^{-1} were transferred to around 970 cm^{-1} coinciding with the Si–O–T. This could refer to the peaks of GGBFS represented at around 970 cm^{-1} [44,45]. Furthermore, the bands between 1420–1490 cm^{-1} represented the vibrations of C–O in attribution to $CaCO_3$ from GGBFS [46], which could also prove that there were Ca elements in Fig. 5b. Moreover, the bands in the region of 1700–3510 cm^{-1} were attributed to the stretching and bending vibrations of O–H and H–O–H from the alkaline solution [47,48].

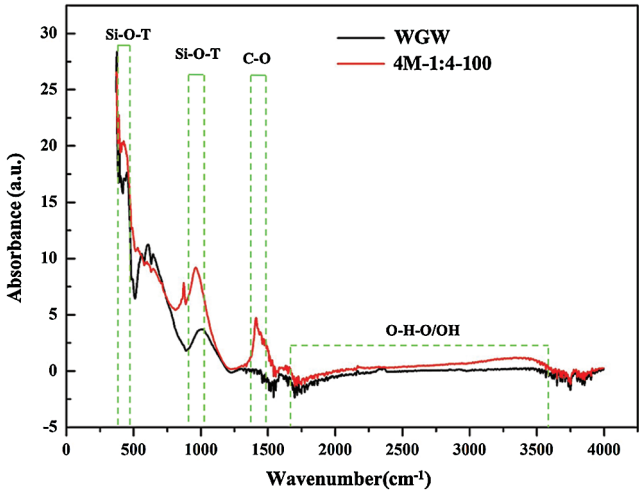

Figure 7: FTIR analysis of WGW and 4M-1:4-100 specimen

3.4 Compressive Strength Test after Freezing–Thawing

Both 2M-1:4-100 and 4M-1:4-100 were tested under 30 freezing–thawing cycles in accordance with the standard; the results of the strength loss are shown in Fig. 8. The compressive strength of 2M-1:4-100 after the freezing–thawing cycles was 25.12 MPa, and the strength loss was only 16.7%. In contrast, the compressive strength of 4M-1:4-100 after the freezing–thawing cycles was 43.24 MPa, and the strength loss was only 14.5%. Furthermore, Fig. 9 illustrates the appearance of the 4M-1:4-100 specimen before and after the test. As can be seen, the appearance did not change apparently after the 30 test cycles. Thus, we inferred from the mechanical properties and the appearance that WGW was feasible for the development of high-strength bricks.

3.5 Toxicity Characteristic Leaching Procedure (TCLP) Results

The toxicity characteristic leaching procedure results of 4M-1:4-100 and the permissible limit of toxic elements are shown in Tab. 4, in order to comprehend whether the geopolymer WGW bricks were eco-friendly or not. The elements detected by the ICP instrument included Pb, Cd, Cr, Cu, Zn, Ba, As, and Hg. The results showed that the concentration of all the elements from 4M-1:4-100 remained undetected, which were lower than the US EPA limit value. As a result, the geopolymer WGW bricks were concluded to be non-toxic construction materials and eco-friendly.

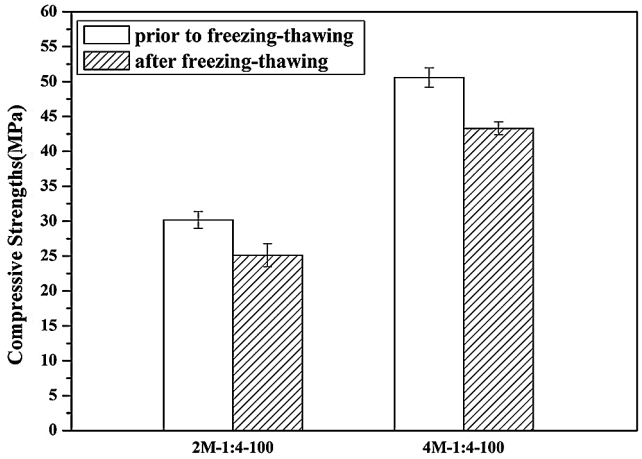

Figure 8: Compressive strength of 2M-1:4-100 and 4M-1:4-100 before and after 30 freezing–thawing cycles

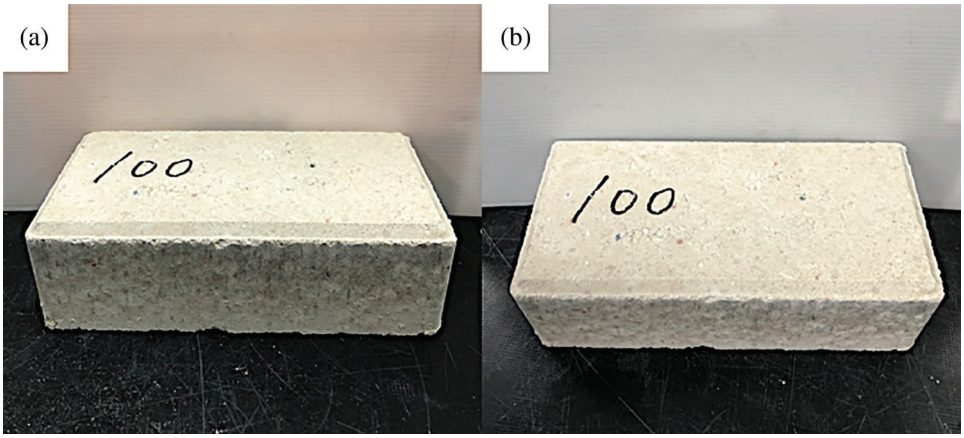

Figure 9: 4M-1:4-100 freezing-thawing specimen: a) before and b) after

Table 4: TCLP test of 4M-1:4-100

Analysis radicals	Concentration of toxic radicals (mg/l)	
	4M-1:4-100	EPA limit
Pb	N.D.	5
Cd	N.D.	1
Cr	N.D.	5
Cu	N.D.	15
Zn	N.D.	–
Ba	N.D.	100
As	N.D.	5
Hg	N.D.	0.02

Note: N.D. - Not Detected.

4 Conclusion

This study revealed that it was feasible to use the WGW to make geopolymer WGW bricks. We investigated the effect of three major factors, namely the press-forming pressure, NaOH concentration, and the ratio of the binder fine-aggregate. From the experimental results, the following conclusions were drawn:

(1) Increasing the press-forming pressure to 100 kgf/cm^2 can make the bricks denser and then eventually enhance the bulk density and the compressive strength.

(2) The geopolymer WGW bricks prepared at the 4M NaOH concentration had higher strength than those prepared at 2M. The maximum compressive strength at the 4M NaOH concentration could reach 56.1 MPa after 28 days. This was attributed to the higher NaOH concentration, which can considerably increase the reaction rate and the strength.

(3) The optimal formulation was composed of 1:4 binder fine-aggregate ratio, 4M NaOH concentration, and 100-kgf/cm^2 pressure. The specimen prepared using the ratio of 1:4 can use further WGW and reached 50.6 MPa after 28 days, which was greater than 32 MPa and thus conformed to the Grade A brick standard of CNS (13295).

(4) The optimal formulation of 4M-1:4-100 was tested under 30 freezing–thawing cycles and toxicity characteristic leaching procedure. The results revealed that the compressive strength was 43.24 MPa and the strength loss was only 14.5%, also it was a non-toxic construction material and eco-friendly.

As a result, this study presented a new feasible method to make geopolymer bricks by using WGWs that not only is more environment friendly but can also replace the conventional fired bricks.

Funding Statement: The authors received no specific funding for this study.

Conflicts of Interest: The authors declare that they have no conflicts of interest to report regarding the present study.

References

1. Kilns, H. Z. Z. (2019). The brick market. https://www.hablakilns.com/the-brick-industry/the-brick-market/.
2. Chen, Y., Zhang, Y., Chen, T., Zhao, Y., Bao, S. (2011). Preparation of eco-friendly construction bricks from hematite tailings. *Construction and Building Materials, 25(4),* 2107–2111. DOI 10.1016/j.conbuildmat.2010.11.025.
3. Lingling, X., Wei, G., Tao, W., Nanru, Y. (2005). Study on fired bricks with replacing clay by fly ash in high volume ratio. *Construction and Building Materials, 19(3),* 243–247. DOI 10.1016/j.conbuildmat.2004.05.017.
4. Eliche-Quesada, D., Sánchez-Martínez, J., Felipe-Sesé, M. A., Infantes-Molina, A. (2017). Silica–calcareous non fired bricks made of biomass ash and dust filter from gases purification. *Waste and Biomass Valorization, 10(2),* 417–431. DOI 10.1007/s12649-017-0056-1.
5. Wu, S. X., Huang, S. S., Tan, C. B., Cai, H. (2012). Application of spent bleaching clay for producing environmental brick. *Applied Mechanics and Materials, 204-208,* 3668–3671. DOI 10.4028/www.scientific.net/AMM.204-208.3668.
6. Yu, H., Zheng, L., Yang, J., Yang, L. (2015). Stabilised compressed earth bricks made with coastal Solonchak. *Construction and Building Materials, 77,* 409–418. DOI 10.1016/j.conbuildmat.2014.12.069.
7. Zheng, Y. (2012). Preparation, properties, formation mechanism of autoclaved bricks from waste foundry sand. *Applied Mechanics and Materials, 174-177,* 697–700. DOI 10.4028/www.scientific.net/AMM.174-177.697.
8. Zhou, J., Yu, D., Shu, Z., Li, T., Chen, Y. et al. (2014). A novel two-step hydration process of preparing cement-free non-fired bricks from waste phosphogypsum. *Construction and Building Materials, 73,* 222–228. DOI 10.1016/j.conbuildmat.2014.09.075.

9. Upoma Saha, M., Hossain, F. (2019). Making non-fired brick using locally produced induction furnace steel slag. *International Conference on Computer, Communication, Chemical, Materials and Electronic Engineering IC4ME2*. Bangladesh University of Engineering and Technology Dhaka, Bangladesh.
10. Huynh, T. P., Nguyen, T. C., Do, N. D., Hwang, C. L., Bui, L. A. T. (2019). Strength and thermal properties of unfired four-hole hollow bricks manufactured from a mixture of cement, low-calcium fly ash and blended fine aggregates. *IOP Conference Series: Materials Science and Engineering, 625,* 012010. DOI 10.1088/1757-899X/625/1/012010.
11. Peng, Y., Peng, X., Yang, M., Shi, H., Wang, W. et al. (2020). The performances of the baking-free bricks of non-sintered wrap-shell lightweight aggregates from dredged sediments. *Construction and Building Materials, 238,* 117587. DOI 10.1016/j.conbuildmat.2019.117587.
12. Zhou, J., Gao, H., Shu, Z., Wang, Y., Yan, C. (2012). Utilization of waste phosphogypsum to prepare non-fired bricks by a novel hydration–recrystallization process. *Construction and Building Materials, 34,* 114–119. DOI 10.1016/j.conbuildmat.2012.02.045.
13. Türkmen, İ., Ekinci, E., Kantarcı, F., Sarıcı, T. (2017). The mechanical and physical properties of unfired earth bricks stabilized with gypsum and Elazığ Ferrochrome slag. *International Journal of Sustainable Built Environment, 6(2),* 565–573. DOI 10.1016/j.ijsbe.2017.12.003.
14. Liu, Z., Chen, Q., Xie, X., Xue, G., Du, F. et al. (2011). Utilization of the sludge derived from dyestuff-making wastewater coagulation for unfired bricks. *Construction and Building Materials, 25(4),* 1699–1706. DOI 10.1016/j.conbuildmat.2010.10.012.
15. Olofinnade, O., Ogara, J., Oyawoye, I., Ede, A., Ndambuki, J. et al. (2019). Mechanical properties of high strength eco-concrete containing crushed waste clay brick aggregates as replacement for sand. *IOP Conference Series: Materials Science and Engineering, 640,* 012046. DOI 10.1088/1757-899x/640/1/012046.
16. Wang, Z., Zhao, C., Zhang, Y., Hua, B., Lu, X. (2019). Study on strength characteristics of straw (EPS particles)-sparse sludge unburned brick. *IOP Conference Series: Materials Science and Engineering, 490(3),* 032005. DOI 10.1088/1757-899x/490/3/032005.
17. Maddalena, R., Roberts, J. J., Hamilton, A. (2018). Can Portland cement be replaced by low-carbon alternative materials? A study on the thermal properties and carbon emissions of innovative cements. *Journal of Cleaner Production, 186,* 933–942. DOI 10.1016/j.jclepro.2018.02.138.
18. Assi, L., Carter, K., Deaver, E., Anay, R., Ziehl, P. (2018). Sustainable concrete: building a greener future. *Journal of Cleaner Production, 198,* 1641–1651. DOI 10.1016/j.jclepro.2018.07.123.
19. Bakharev, T. (2005). Geopolymeric materials prepared using Class F fly ash and elevated temperature curing. *Cement and Concrete Research, 35(6),* 1224–1232. DOI 10.1016/j.cemconres.2004.06.031.
20. Ismail, M., Yusuf, T. O., Noruzman, A. H., Hassan, I. O. (2013). Early strength characteristics of palm oil fuel ash and metakaolin blended geopolymer mortar. *Advanced Materials Research, 690–693,* 1045–1048. DOI 10.4028/www.scientific.net/AMR.690-693.1045.
21. Lee, W. K. W., van Deventer, J. S. J. (2002). The effect of ionic contaminants on the early-age properties of alkali-activated fly ash-based cements. *Cement and Concrete Research, 32(4),* 577–584. DOI 10.1016/S0008-8846(01)00724-4.
22. Amin, S. K., El-Sherbiny, S. A., El-Magd, A. A. M. A., Belal, A., Abadir, M. F. (2017). Fabrication of geopolymer bricks using ceramic dust waste. *Construction and Building Materials, 157,* 610–620. DOI 10.1016/j.conbuildmat.2017.09.052.
23. Youssef, N., Rabenantoandro, A. Z., Dakhli, Z., Chapiseau, C., Waendendries, F. et al. (2019). Reuse of waste bricks: A new generation of geopolymer bricks. *SN Applied Sciences, 1(10),* 397. DOI 10.1007/s42452-019-1209-6.
24. Hwang, C. L., Huynh, T. P., Risdianto, Y. (2016). An application of blended fly ash and residual rice husk ash for producing green building bricks. *Journal of the Chinese Institute of Engineers, 39(7),* 850–858. DOI 10.1080/02533839.2016.1191376.
25. Ahmari, S., Zhang, L. (2012). Production of eco-friendly bricks from copper mine tailings through geopolymerization. *Construction and Building Materials, 29,* 323–331. DOI 10.1016/j.conbuildmat.2011.10.048.

26. Madani, H., Ramezanianpour, A. A., Shahbazinia, M., Ahmadi, E. (2020). Geopolymer bricks made from less active waste materials. *Construction and Building Materials, 247,* 118441. DOI 10.1016/j.conbuildmat.2020.118441.
27. Apithanyasai, S., Supakata, N., Papong, S. (2020). The potential of industrial waste: using foundry sand with fly ash and electric arc furnace slag for geopolymer brick production. *Heliyon, 6(3),* e03697. DOI 10.1016/j.heliyon.2020.e03697.
28. Kaur, M., Singh, J., Kaur, M. (2018). Synthesis of fly ash based geopolymer mortar considering different concentrations and combinations of alkaline activator solution. *Ceramics International, 44(2),* 1534–1537. DOI 10.1016/j.ceramint.2017.10.071.
29. Kaur, K., Singh, J., Kaur, M. (2018). Compressive strength of rice husk ash based geopolymer: The effect of alkaline activator. *Construction and Building Materials, 169,* 188–192. DOI 10.1016/j.conbuildmat.2018.02.200.
30. CNS (2010). Compressed concrete paving units. https://www.cnsonline.com.tw/.
31. CNS (2015). Method of test for obtaining and testing drilled cored and sawed beams of concrete. https://www.cnsonline.com.tw/.
32. CNS (2016). Method of test for compression testing machines. https://www.cnsonline.com.tw/.
33. CNS (2015). Method of test for apparent porosity, water absorption and specific gravity of refractory bricks. https://www.cnsonline.com.tw/.
34. Bouchhima, L., Rouis, M. J., Choura, M. (2017). A study of compaction pressure influence on properties of phosphogypsum-based bricks. *Romanian Journal of Materials, 47,* 476–483.
35. Rifaai, Y., Yahia, A., Mostafa, A., Aggoun, S., Kadri, E. H. (2019). Rheology of fly ash-based geopolymer: effect of NaOH concentration. *Construction and Building Materials, 223,* 583–594. DOI 10.1016/j.conbuildmat.2019.07.028.
36. Singh, N. B., Saxena, S. K., Kumar, M., Rai, S. (2019). Geopolymer cement: synthesis, characterization, properties and applications. *Materials Today: Proceedings, 15,* 364–370. DOI 10.1016/j.matpr.2019.04.095.
37. Rattanasak, U., Chindaprasirt, P. (2009). Influence of NaOH solution on the synthesis of fly ash geopolymer. *Minerals Engineering, 22(12),* 1073–1078. DOI 10.1016/j.mineng.2009.03.022.
38. Arellano-Aguilar, R., Burciaga-Díaz, O., Gorokhovsky, A., Escalante-García, J. I. (2014). Geopolymer mortars based on a low grade metakaolin: Effects of the chemical composition, temperature and aggregate: binder ratio. *Construction and Building Materials, 50,* 642–648. DOI 10.1016/j.conbuildmat.2013.10.023.
39. Joseph, B., Mathew, G. (2012). Influence of aggregate content on the behavior of fly ash based geopolymer concrete. *Scientia Iranica, 19(5),* 1188–1194. DOI 10.1016/j.scient.2012.07.006.
40. Gábor, M., Ádám, R., Zoltán, M., Roland, S., Imre, G. et al. (2014). Synergetic use of lignite fly ash and metallurgical converter slag in geopolymer concrete. *Mining Science, 21,* 43–55. DOI 10.5277/ms142104.
41. Richardson, I. G., Brough, A. R., Groves, G. W., Dobson, C. M. (1994). The characterization of hardened alkali-activated blast-furnace slag pastes and the nature of the calcium silicate hydrate (C–S–H) phase. *Cement and Concrete Research, 24(5),* 813–829. DOI 10.1016/0008-8846(94)90002-7.
42. Ismail, I., Bernal, S. A., Provis, J. L., San Nicolas, R., Hamdan, S. et al. (2014). Modification of phase evolution in alkali-activated blast furnace slag by the incorporation of fly ash. *Cement and Concrete Composites, 45,* 125–135. DOI 10.1016/j.cemconcomp.2013.09.006.
43. Yang, T., Yao, X., Zhang, Z., Wang, H. (2012). Mechanical property and structure of alkali-activated fly ash and slag blends. *Journal of Sustainable Cement-Based Materials, 1(4),* 167–178. DOI 10.1080/21650373.2012.752621.
44. García Lodeiro, I., Macphee, D. E., Palomo, A., Fernández-Jiménez, A. (2009). Effect of alkalis on fresh C–S–H gels. FTIR analysis. *Cement and Concrete Research, 39(3),* 147–153. DOI 10.1016/j.cemconres.2009.01.003.
45. Hajimohammadi, A., Provis, J. L., van Deventer, J. S. J. (2010). Effect of alumina release rate on the mechanism of geopolymer gel formation. *Chemistry of Materials, 22(18),* 5199–5208. DOI 10.1021/cm101151n.
46. Puligilla, S., Mondal, P. (2013). Microstructural changes responsible for hardening of fly ash-slag geopolymers studied through infrared spectroscopy. In *Geopolymer Binder Systems, STP 1566*, Leslie Struble, James K. Hicks, eds., ASTM International, pp. 21–33. DOI 10.1520/STP156620120084.

47. Tuyan, M., Andiç-Çakir, Ö., Ramyar, K. (2018). Effect of alkali activator concentration and curing condition on strength and microstructure of waste clay brick powder-based geopolymer. *Composites Part B: Engineering, 135,* 242–252. DOI 10.1016/j.compositesb.2017.10.013.

48. Abdollahnejad, Z., Pacheco-Torgal, F., Aguiar, J. B., Jesus, C. (2014). Durability performance of fly ash based one-part geopolymer mortars. *Key Engineering Materials, 634,* 113–120. DOI 10.4028/www.scientific.net/KEM.634.113.